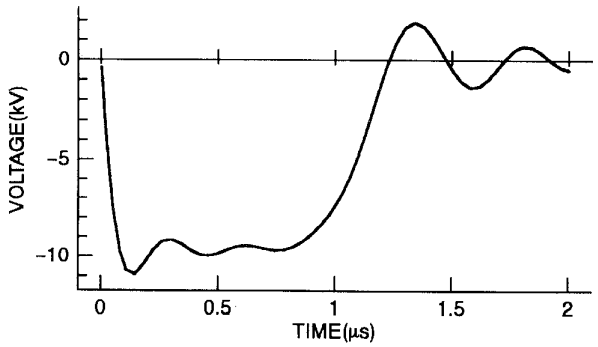

Fig. 6. Simulation result of output pulse in $L = 2$ H case with a five-section uniform-line PFN when t_0 equals 0.566 ms.

no difference between the two simulation results obtained with the three-section and the five-section uniform-line PFN's.

VI. Conclusion

A technique of controlling rapidly the output peak voltage of a line-type pulse modulator has been proposed, and the analytical results of the circuit have also been given. The results calculated in the two cases with different control ranges of the output peak voltage and the results of simulation in the two cases represent well the feasibility of this technique. The technique of rapidly changing pulse voltage is also applicable to the low voltage pulse circuits such as transistor pulse circuits. In a high power pulse modulator in which the impedance of a PFN is generally selected to be low to obtain large current, the additional switch tube cannot play a part of the thyratron because of its relatively high internal resistance. However, in a low voltage pulse circuit, the additional switch transistor can do the work of both the "thyratron" transistor (e.g., SCR) and the additional switch transistor, because relatively high impedance of a PFN is acceptable. So, in such an application, the thyratron transistor can be removed from the circuit.

Investigating the effects on the circuit operation of nonlinearity of the charging element which is usually encountered in the iron-core inductor is a subject for future study.

Since the circuit performance of controlling peak voltages is limited by the handling voltage capability of the available switch tube, it is necessary to develop effective high voltage switching devices in order to respond to various design demands.

Acknowledgment

The author wishes to thank A. Kawasaki of the graduate course of Hiroshima Institute of Technology for his assistance with the computer simulations.

References

[1] G. T. Coate and L. R. Swain, *High-Power Semiconductor-Magnetic Pulse Generators*. Cambridge, MA: MIT Press, 1966, Res. Monograph 39.

[2] T. Kondoh and K. Nakatsuka, "Solid state pulse modulator for radar," *Mitsubishidenki Giho*, vol. 49, no. 5, pp. 409–413, May 1975.

[3] G. N. Glasoe and J. V. Lebacqz, Ed., *Pulse Generators*. New York: McGraw-Hill, 1948, part I and II.

[4] K. Nakatsuka, "Effects of stray capacitance on the performance of a short-pulse modulator—Evaluating by drawing," *Trans. IECE Japan*, vol. J68-B, no. 1, pp. 143–144, Jan. 1985.

[5] ——, "Analysis of the effects of shunt capacitance on the performance of pulse modulators," *IEEE Circuits Syst.*, vol. 36, pp. 1105–1110, Aug. 1989.

[6] ——, "Output control of the line-type pulser by time-voltage conversion," *Trans. IEICE Japan*, vol. J76-B-II, no. 3, pp. 184–186, Mar. 1993.

Synchronization of Chua's Circuits with Time-Varying Channels and Parameters

Leon O. Chua, Tao Yang, Guo-Qun Zhong, and Chai Wah Wu

***Abstract*—In this brief, we study the use of adaptive controllers to maintain the synchronization of two Chua's circuits with time-varying channel and time-varying parameters. Both simulation results and experimental results are provided to verify the operation of the designs.**

I. Introduction

Because of its potential applications to spread spectrum communication, the synchronization of chaotic systems has been studied extensively both in theory and in experiments [1]–[17]. However, in almost all of the previous works, the driving and the driven chaotic systems are assumed to be identical and their parameters are assumed to be time-invariant. The channel through which the transmitted signal is transmitted is also assumed to be time-invariant. The above assumptions limit its applicability in practical systems.

So far, all chaos-based communication systems use chaotic systems both as transmitters and receivers. The transmitter generates a chaotic signal which is used to encode the message signal in different ways, for example: chaotic masking [1]–[3], parameter modulation [8], [9] and state variable modulation [5], [6], [17]. Chaotic masking is not very secure if the message is directly added onto the chaotic masking signal. The authors of [4] and [19] had demonstrated that the smaller the message signal is, the lower the degree of security will be. Chaotic switching is the easiest form of parameter modulation and it was also shown to have a low degree of security [20] if the parameters of the transmitter are not chosen carefully. State variable modulation uses a functional of the message signal to modulate the state variables of the transmitter and hides the message signal, which is usually a narrow-band signal, into the broad-band chaotic signal.

Manuscript received October 4, 1995; revised February 13, 1996. This paper was recommended by Associate Editor T. Endo.

L. O. Chua and C. W. Wu are with the Electronics Research Laboratory and Department of Electrical Engineering and Computer Sciences, University of California, Berkeley, CA 94720 USA.

T. Yang is with the Electronics Research Laboratory and Department of Electrical Engineering and Computer Sciences, University of California, Berkeley, CA 94720 USA, on leave from the Department of Automatic Control Engineering, Shanghai University of Technology, Shanghai 200072, P. R. China.

G.-Q. Zhong is with the Electronics Research Laboratory and Department of Electrical Engineering and Computer Sciences, University of California, Berkeley, CA 94720 USA, on leave from the Guangzhou Institute of Electronic Technology, Academia Sinica, Guangzhou 510070, P. R. China.

Publisher Item Identifier S 1057-7122(96)07600-3.

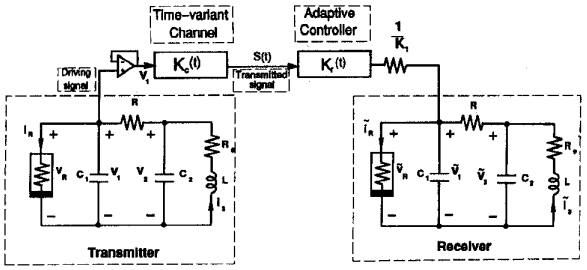

Fig. 1. The synchronization scheme of two Chua's circuits by using v_1 in a unidirectional driving configuration.

The transmitted signal is then transmitted to the receiver, which is an identical chaotic system. The transmitted signal will synchronize the receiver to the transmitter to obtain a replica of the chaotic masking signal.

Most of the methods presented so far require that the parameters of the transmitter and the receiver are identical, and the channel is time-invariant. Our experimental results indicate that a time-varying channel can desynchronize the system.

In this brief, we use adaptive controllers to maintain the synchronization between the transmitter and the receiver when the parameters of the transmitter are time-varying or the channel is memoryless and time-varying. We used Chua's circuits as our driving and driven system. The feedback into the adaptive controller is the synchronization error, which measures the degree of de-synchronization between the transmitter and receiver.

The organization of this brief is as follows. In Section II, adaptive controllers are presented which compensate the time-varying channel gain. In Section III, adaptive controllers are presented which compensate the time-varying parameters. In Section IV, experimental results are presented.

II. Adaptive Controllers for Time-Varying Channel Compensation

In this brief, all the results are based on Chua's circuit [18], [21], which exhibits a family of chaotic attractors and can be easily implemented in hardware. Chua's circuit consists of a linear inductor L, a linear resistor R, two linear capacitors C_1 and C_2 and a nonlinear resistor—the Chua's diode N_R. The state equations for Chua's circuit are given by

$$\begin{cases} \frac{dv_1}{dt} = \frac{1}{C_1}[G(v_2 - v_1) - f(v_1)] \\ \frac{dv_2}{dt} = \frac{1}{C_2}[G(v_1 - v_2) + i_3] \\ \frac{di_3}{dt} = \frac{1}{L}[-v_2 - R_0 i_3] \end{cases} \tag{1}$$

where v_1, v_2 and i_3 are the voltage across C_1, the voltage across C_2 and the current through L, respectively. We set $G = \frac{1}{R}$. The term $R_0 i_3$ is added to account for the small resistance of the inductor in the physical circuit. $f(v_1)$, the piece-wise linear $v - i$ characteristic of the Chua's diode, is given by

$$f(v_1) = G_b v_1 + \frac{1}{2}(G_a - G_b)(|v_1 + E| - |v_1 - E|) \tag{2}$$

where E is the breakpoint voltage of the Chua's diode.

We use the synchronization scheme shown in Fig. 1 [12]. The state equations are given by

$$\begin{cases} \frac{dv_1}{dt} = \frac{1}{C_1}[G(v_2 - v_1) - f(v_1)] \\ \frac{dv_2}{dt} = \frac{1}{C_2}[G(v_1 - v_2) + i_3] \\ \frac{di_3}{dt} = \frac{1}{L}[-v_2 - R_0 i_3] \end{cases} \tag{3}$$

$$\begin{cases} \frac{d\tilde{v}_1}{dt} = \frac{1}{C_1}[G(\tilde{v}_2 - \tilde{v}_1) - f(\tilde{v}_1) + K_1(s(t) - \tilde{v}_1)] \\ \frac{d\tilde{v}_2}{dt} = \frac{1}{C_2}[G(\tilde{v}_1 - \tilde{v}_2) + \tilde{i}_3] \\ \frac{d\tilde{i}_3}{dt} = \frac{1}{L}[-\tilde{v}_2 - R_0 \tilde{i}_3] \end{cases} \tag{4}$$

where $s(t) = K_c(t)v_1$, and $K_c(t)$ is the time-varying gain of the channel. Constant unity gain channel corresponds to $K_c(t) = 1$.

In this section we study how to compensate for the time-varying channel gain $K_c(t)$. In the driven system, we construct an adaptive gain $K_r(t)$ such that $K_c(t)K_r(t) \to 1$ as $t \to \infty$ to maintain the synchronization. Then the driven system should be rewritten as

$$\begin{cases} \frac{d\tilde{v}_1}{dt} = \frac{1}{C_1}[G(\tilde{v}_2 - \tilde{v}_1) - f(\tilde{v}_1) + K_1(K_r(t)s(t) - \tilde{v}_1)] \\ \frac{d\tilde{v}_2}{dt} = \frac{1}{C_2}[G(\tilde{v}_1 - \tilde{v}_2) + \tilde{i}_3] \\ \frac{d\tilde{i}_3}{dt} = \frac{1}{L}[-\tilde{v}_2 - R_0 \tilde{i}_3] \end{cases} \tag{5}$$

The dynamics of $K_r(t)$ is given by one of the following adaptive controllers:

Controller #1

$$\dot{K}_r(t) = -k_1(K_r(t)|s(t)| - |\tilde{v}_1|) \tag{6}$$

Controller #2

$$\dot{K}_r(t) = -k_1(K_r(t)s^2(t) - s(t)\tilde{v}_1) \tag{7}$$

Controller #3

$$\begin{aligned} \dot{K}_r(t) &= -k_1 \operatorname{sgn}\left(\frac{\partial \dot{\tilde{v}}_1}{\partial K_r}\right)(K_r(t)s(t) - \tilde{v}_1) \\ &= -k_1 \operatorname{sgn}(K_1 s(t))(K_r(t)s(t) - \tilde{v}_1). \end{aligned} \tag{8}$$

Controller #2 is similar to the LMS adaptive controller and controller #3 is a simple form of the adaptive controllers discussed in [22] and [23].

In our simulations, the parameters of Chua's circuit are given by $C_1 = 5.56$ nF, $C_2 = 50$ nF, $G = 0.700\,28$, $L = 7.14$ mH, $R_0 = 0$ Ω, $G_a = -0.8$ mS, $G_b = -0.5$ mS, $E = 1$ V, $K_1 = 0.01$. The Chua's circuit exhibits a double scroll Chua's attractor for these parameters. We choose the synchronization error to be $v_1 - \tilde{v}_1$. In all of our simulations, the initial conditions of the transmitter and the receiver are $(v_1(0),\ v_2(0),\ i_3(0)) = (-0.2$ V, $-0,02$ V, 0.1 mA) and $(\tilde{v}_1(0),\ \tilde{v}_2(0),\ \tilde{i}_3(0)) = (0.02$ V, -0.12 V, -0.1 mA), respectively. So the transmitter and the receiver are initially desynchronized. The fourth order Runge–Kutta method with fixed step-size $h = 10^{-6}$ s is used to simulate the system.

Fig. 2 shows the simulation results when $K_c(t)$ is a sinusoidal function as follows

$$K_c(t) = 0.5 - 0.1\sin(75\pi t) \tag{9}$$

and controller #1 is used with $k_1 = 10^6$.

Fig. 2(a) shows $K_c(t)$, $K_r(t)$ and $K_c(t)K_r(t)$. We can see that $K_r(t)$ asymptotically approaches $\frac{1}{K_c(t)}$, and the settling time is about 0.6 ms. Fig. 2(b) shows the synchronization error $v_1(t) - \tilde{v}_1(t)$. For comparison, the synchronization error in the case when no adaptive controller is used is shown in Fig. 2(c). One can see that the synchronization error is reduced significantly by using the adaptive controller. When controllers #2 and #3 are used, the simulation results are almost the same.

When the coupling factor K_1 becomes too small, the transmitter and he receiver will be desynchronized even when the channel has a unit gain $K_c(t) = 1$ for all times. Fig. 3(a) shows this de-synchronization with $K_1 = 0.0005$. However, we find that the adaptive controllers used can also compensate for this kind of desynchronization. Fig. 3(b) shows the simulation result when $K_c(t) = 1$ and $K_1 = 0.0005$, and controller #1 with $k_1 = 10^6$ is used. We see that the synchronization error approaches 0.

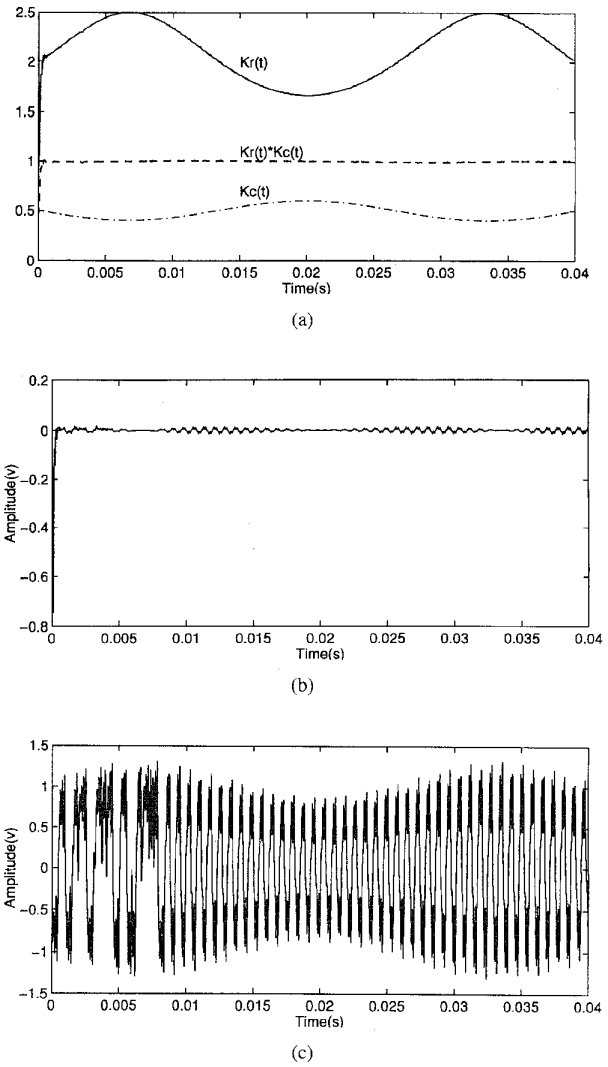

Fig. 2. Synchronization of Chua's circuits when the channel gain $K_c(t)$ is a sinusoidal function and controller #1 is used. (a) The channel gain $K_c(t)$, gain of adaptive controller $K_r(t)$ and the product $K_c(t)K_r(t)$. (b) The synchronization error $(v_1 - \tilde{v}_1)$ when adaptive controller #1 is used. (c) The synchronization error $(v_1 - \tilde{v}_1)$ without using adaptive controller.

III. Adaptive Controller for Time-Varying Parameter Compensation

Parameter mismatch can also result in the loss of synchronization of the system shown in Fig. 1. Although the synchronization is robust in the sense that it can tolerate some parameter mismatch [10], the authors of [5] gave an experimental example showing that a 1% resistor mismatch can sharply reduce the quality of the received signal.

In this section, we study the synchronization in the cases where the parameters of the transmitter are time-varying. In this case, we rewrite the driving system as follows:

$$\begin{cases} \frac{dv_1}{dt} = \frac{K_{C_1}(t)}{C_1}[K_G(t)G(v_2 - v_1) - f(v_1)] \\ \frac{dv_2}{dt} = \frac{K_{C_2}(t)}{C_2}[K_G(t)G(v_1 - v_2) + i_3] \\ \frac{di_3}{dt} = \frac{K_L(t)}{L}[-v_2 - (K_{R_0}(t) + R_0)i_3] \end{cases} \tag{10}$$

where $K_{C_1}(t)$, $K_{C_2}(t)$, $K_L(t)$, $K_{R_0}(t)$ and $K_G(t)$ are the time-varying factors of the parameters C_1, C_2, L, R_0 and G, respectively.

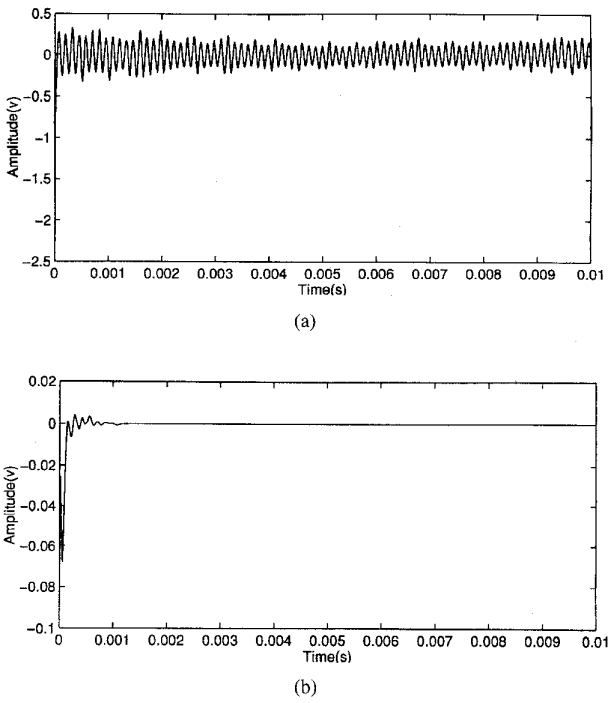

Fig. 3. (a) The synchronization error $(v_1 - \tilde{v}_1)$ when channel gain $K_c(t) = 1$ and a weak coupling factor $K_1 = 0.0005$ is used. No controller is used. (b) The synchronization error $(v_1 - \tilde{v}_1)$ when the channel gain $K_c(t)$ is 1 and a weak coupling factor $K_1 = 0.0005$ is used. Controller #1 is used.

The driven system is as follows:

$$\begin{cases} \frac{d\tilde{v}_1}{dt} = \frac{\tilde{K}_{C_1}(t)}{C_1}[\tilde{K}_G(t)G(\tilde{v}_2 - \tilde{v}_1) - f(\tilde{v}_1) + K_1(v_1 - \tilde{v}_1)] \\ \frac{d\tilde{v}_2}{dt} = \frac{\tilde{K}_{C_2}(t)}{C_2}[\tilde{K}_G(t)G(\tilde{v}_1 - \tilde{v}_2) + \tilde{i}_3 + K_1(v_1 - \tilde{v}_1)] \\ \frac{d\tilde{i}_3}{dt} = \frac{\tilde{K}_L(t)}{L}[-\tilde{v}_2 - (\tilde{K}_{R_0}(t) + R_0)\tilde{i}_3 + K_1(v_1 - \tilde{v}_1)] \end{cases} \tag{11}$$

where $\tilde{K}_{C_1}(t)$, $\tilde{K}_{C_2}(t)$, $\tilde{K}_L(t)$, $\tilde{K}_{R_0}(t)$ and $\tilde{K}_G(t)$ are compensating adjustments of the parameters C_1, C_2, L, R_0 and G, respectively, which are adaptively modified by using the following adaptive controllers. In this paper, we consider the cases when only one parameter is time-varying at a time. The adaptive controllers used are similar in form to those used in [22] and [23].

A. Compensating for K_G

The controller is chosen as

$$\begin{aligned} \dot{\tilde{K}}_G(t) &= k_1 \operatorname{sgn}\left(\frac{\partial \dot{\tilde{v}}_1}{\partial \tilde{K}_G}\right)(v_1 - \tilde{v}_1) \\ &= k_1 \operatorname{sgn}\left(\frac{1}{C_1}G(\tilde{v}_2 - \tilde{v}_1)\right)(v_1 - \tilde{v}_1) \end{aligned} \tag{12}$$

The simulation results are shown in Fig. 4 with $k_1 = 10^6$. $K_G(t)$ is defined by the following sinusoidal function.

$$1.1 - 0.05 \sin\left(\frac{15\pi}{2}t\right) \tag{13}$$

Fig. 4(a) shows $K_G(t)$(dashed line) and $\tilde{K}_G(t)$(solid line). One can see that $\tilde{K}_G(t)$ asymptotically approaches $K_G(t)$ with a settling time of about 3 ms. Fig. 4(b) shows the synchronization error. Note in Fig. 4(a) that from 45.5 to 63 ms, $\tilde{K}_G(t)$ is almost constant while $K_G(t)$ decreases. This is because in the parameter range corresponding to the waveform of $K_G(t)$ during 45.5 ms to 63 ms, the synchronization is maintained even though $\tilde{K}_G(t) \neq K_G(t)$. In

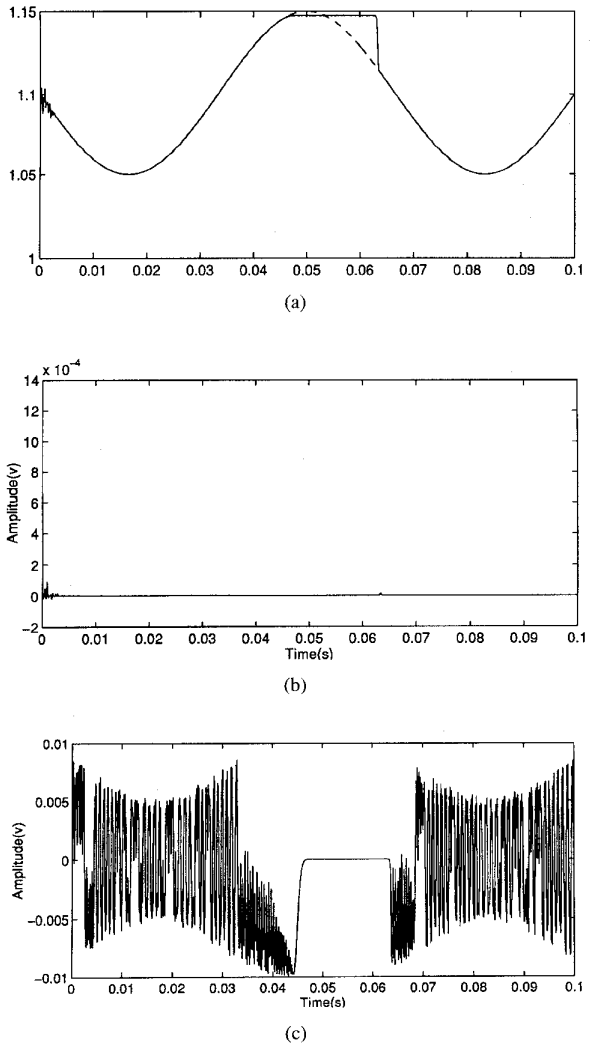

Fig. 4. Synchronization of Chua's circuits when G is a sinusoidal function of time. (a) $K_G(t)$ and $\tilde{K}_G(t)$. (b) The synchronization error $(v_1 - \tilde{v}_1)$ when the adaptive controller is used. (c) The synchronization error $(v_1 - \tilde{v}_1)$ without the adaptive controller.

Fig. 4(c) we show the synchronization error without the adaptive controller and we can see that in the period 45.5 to 63 ms the synchronization error is small.

B. Compensating for K_{C_1}

In this case, the controller used is

$$\dot{\tilde{K}}_{C_1}(t) = k_1 \operatorname{sgn}\left(\frac{\partial \dot{\tilde{v}}_1}{\partial \tilde{K}_{C_1}}\right)(v_1 - \tilde{v}_1) = k_1 \operatorname{sgn}\left(\frac{1}{C_1}[G(\tilde{v}_2 - \tilde{v}_1) - f(\tilde{v}_1) + K_1(v_1 - \tilde{v}_1)]\right) \times (v_1 - \tilde{v}_1). \quad (14)$$

The simulation results are shown in Fig. 5 with $k_1 = 2 \times 10^6$. $K_{C_1}(t)$ is the sinusoidal function given in (13). From Fig. 5(a) one can see that $\tilde{K}_{C_1}(t)$ asymptotically approaches $K_{C_1}(t)$ with a settling time of about 1 ms. Fig. 5(b) shows the synchronization error.

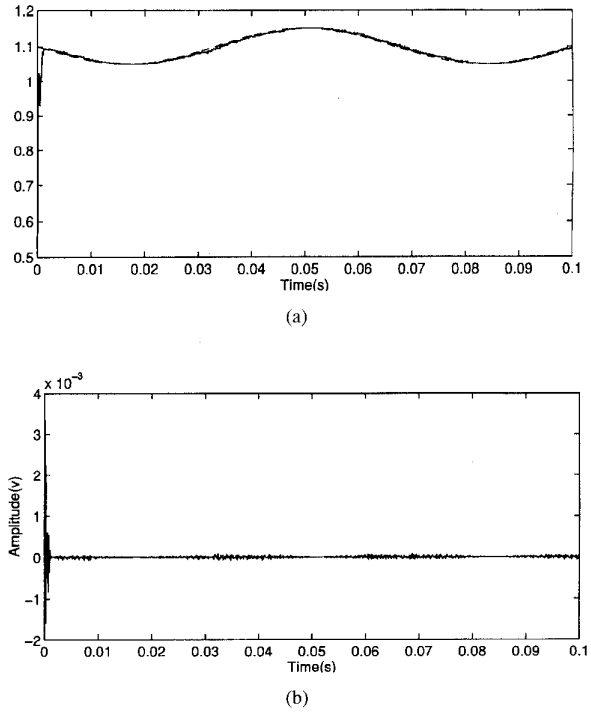

Fig. 5. Synchronization of Chua's circuits when C_1 is a sinusoidal function of time. (a) $K_{C_1}(t)$ and $\tilde{K}_{C_1}(t)$. (b) The synchronization error $(v_1 - \tilde{v}_1)$.

C. Compensating for K_{C_2}

In this case, the controller is

$$\dot{\tilde{K}}_{C_2}(t) = k_1 \operatorname{sgn}\left(\frac{\partial \dot{\tilde{v}}_2}{\partial \tilde{K}_{C_2}}\right)(v_1 - \tilde{v}_1) = k_1 \operatorname{sgn}\left(\frac{1}{C_2}[G(\tilde{v}_1 - \tilde{v}_2) + \tilde{i}_3 + K_1(v_1 - \tilde{v}_1)]\right) \times (v_1 - \tilde{v}_1). \quad (15)$$

The simulation results are similar to those shown in Fig. 5 with $k_1 = 10^6$ and a settling time of about 2 ms.

D. Compensating for K_L

In this case, the controller is

$$\dot{\tilde{K}}_L(t) = k_1 \operatorname{sgn}\left(\frac{\partial \dot{\tilde{i}}_3}{\partial \tilde{K}_L}\right)(v_1(t) - \tilde{v}_1) = k_1 \operatorname{sgn}\left(\frac{1}{L}[-\tilde{v}_2 - R_0\tilde{i}_3 + K_1(v_1 - \tilde{v}_1)]\right) \times (v_1 - \tilde{v}_1). \quad (16)$$

The simulation results are similar to those shown in Fig. 5 with $k_1 = 10^6$ and a settling time of about 2 ms.

E. Compensating for K_{R_0}

In this case, the controller is

$$\dot{\tilde{K}}_{R_0}(t) = k_1 \operatorname{sgn}\left(\frac{\partial \dot{\tilde{i}}_3}{\partial \tilde{K}_{R_0}}\right)(v_1(t) - \tilde{v}_1) = k_1 \operatorname{sgn}\left(-\frac{\tilde{i}_3}{L}\right)(v_1 - \tilde{v}_1). \quad (17)$$

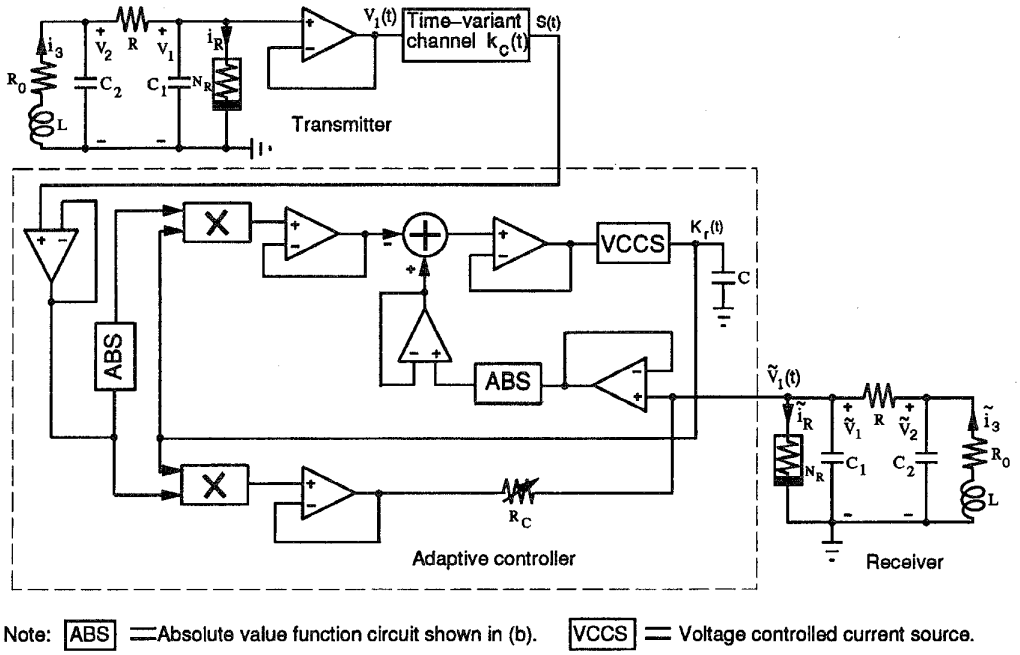

(a)

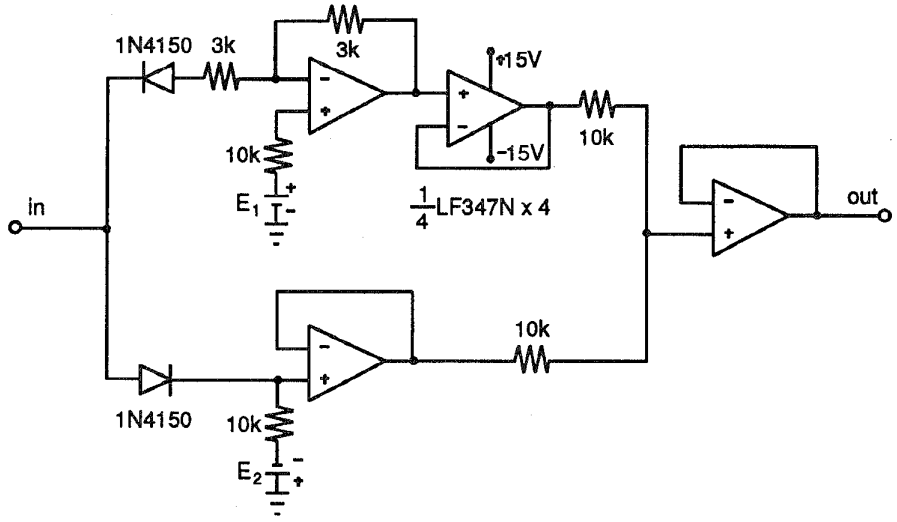

(b)

Fig. 6. (a) Schematic diagram of the experimental circuit for studying the synchronization between two identical Chua's circuits under a time-varying channel. The equations of the adaptive controller is given by (6). (b) Circuit with the absolute value transfer function.

The simulation results are similar to those shown in Fig. 5 with $k_1 = 10^8$ and a settling time of about 1.5 ms.

From the simulation results, we find the frequency of time-varying properties of parameters should be small enough ($\frac{1}{180}$ of the natural frequency of chaotic signal in our simulations), or else the adaptive controllers may not compensate the time-varying parameters.

IV. Experimental Results

In this section we supplement the computer simulation results with experimental results from a physical circuit implementation. The circuit diagram of the system used to study the synchronization between two Chua's circuits when the channel is time-varying is shown in Fig. 6. In our experiments, both Chua's circuits are identical and have the following parameters: $C_1 = 6.8$ nF, $C_2 = 68$ nF, $L = 18.4$ mH, $R_0 = 12\ \Omega$, $R = 1.98$ kΩ, $G_a = -0.73$ mS, $G_b = -0.4$ mS, $E = 1.8$ V, $R_C = 3.8$ kΩ, where R_C is the coupling resistor, which satisfies $K_1 = \frac{1}{R_C}$.

The circuit parameters we used exhibits the Double Scroll Chua's attractor. When the channel gain is 1, the transmitter and the receiver are synchronized.

When the channel gain drops to $K_c(t) = 0.65$, we find that the transmitter and the receiver are desynchronized. The relation between the voltages $v_2(t)$ and $\tilde{v}_2(t)$ is shown in Fig. 7.

Next we use the the adaptive controller as in (6), which is implemented using the circuit shown in Fig. 6 to compensate for the channel gain which is set at $K_c(t) = 0.65$. The

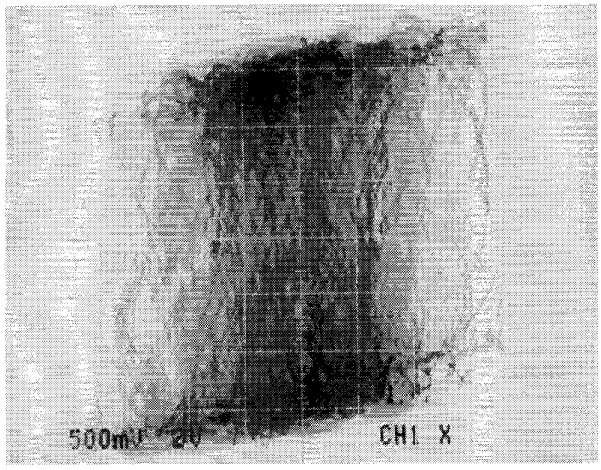

Fig. 7. When the channel gain drops to 0.65, the transmitter and the receiver are desynchronized. No adaptive controller is used. The relationship between v_2 and $\tilde{v}_2$.

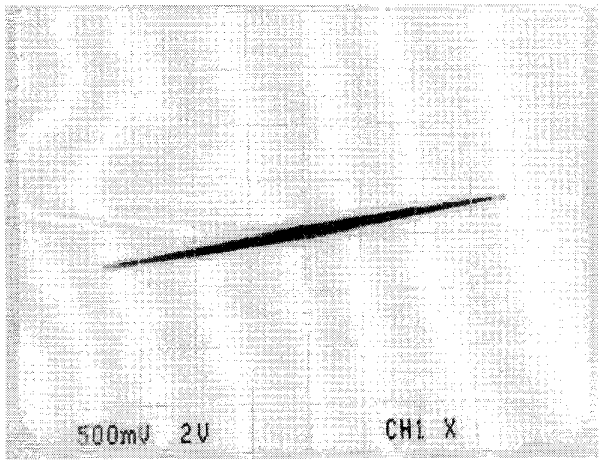

Fig. 8. The adaptive controller in Fig. 6 is used to compensate for the channel gain of 0.65. The relationship between v_2 and $\tilde{v}_2$.

relation between voltages $v_2(t)$ and $\tilde{v}_2(t)$ is shown in Fig. 8. One can see that the synchronization is restored. Comparing the results shown in Fig. 8 with those shown in Fig. 7, one can see that the effect of the adaptive controller is very significant.

Next, we study the effect of our controller under a weak coupling condition. In this case, the coupling resistor is 4.46 kΩ, and as shown in Fig. 9(a), this coupling without the aid of the controller is not big enough to synchronize the transmitter and the receiver even when a unity channel gain is used. In Fig. 9(b), we show the synchronization when the channel gain drops to 0.65 and the controller is used.

V. Conclusion

We have shown how two Chua's circuits can synchronize in the cases where the channel gain and the parameters are time-varying by using adaptive controllers in the receiver to compensate for the time-varying properties of the transmitter and the channel.

Both simulation results and experimental results are presented for the proposed schemes. These results also show that the adaptive controllers can compensate for the weak coupling between the two circuits. These results show that our methods can be useful for developing practical chaotic spread-spectrum communication systems.

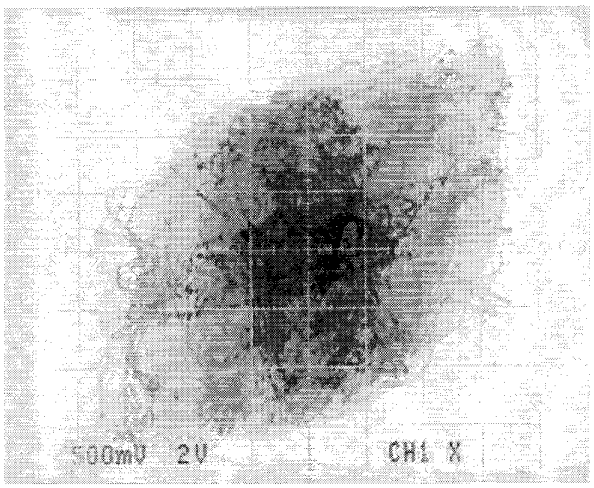

(a)

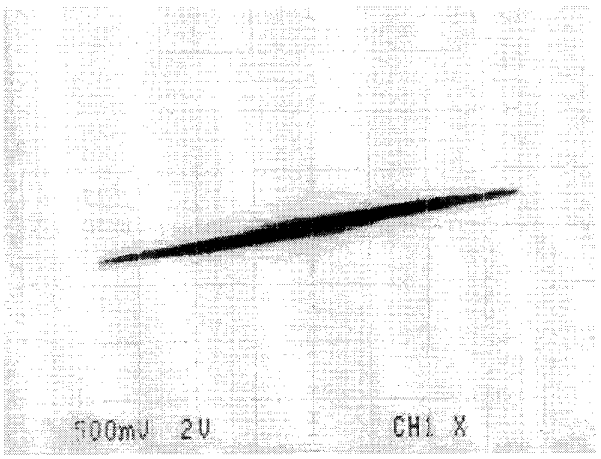

(b)

Fig. 9. The adaptive controller in Fig. 6 can also compensate the de-synchronization caused by weak coupling. (a) The relationship between v_2 and $\tilde{v}_2$ shows the de-synchronization when the coupling resistor is 4.46 kΩ with a unity channel gain. No adaptive controller is used. (b) The relationship between v_2 and $\tilde{v}_2$ shows synchronization when the adaptive controller is used to compensate for the weak coupling factor with a channel gain of 0.65.

References

[1] L. Kocarev, K. S. Halle, K. Eckert, L. O. Chua, and U. Parlitz, "Experimental demonstration of secure communications via chaotic synchronization," *Int. J. Bifurc. Chaos*, vol. 2, no. 3, pp. 709–713, 1992.

[2] K. M. Cuomo and A. V. Oppenheim, "Synchronization of Lorenz-based chaotic circuits with applications to communications," *IEEE Trans. Circuits Syst.*, vol. 40, pp. 626–633, Oct. 1993.

[3] R. Lozi and L. O. Chua, "Secure communications via chaotic synchronization II: Noise reduction by cascading two identical receivers," *Int. J. Bifurc. Chaos*, vol. 3, pp. 1319–1325, 1993.

[4] K. M. Short, "Steps toward unmasking secure communications," *Int. J. Bifurc. Chaos*, vol. 4, pp. 959–977, 1994.

[5] K. S. Halle, C. W. Wu, M. Itoh, and L. O. Chua, "Spread spectrum communication through modulation of chaos," *Int. J. Bifurc. Chaos*, vol. 3, no. 2, pp. 469–477, 1993.

[6] C. W. Wu and L. O. Chua, "A simple way to synchronize chaotic systems with applications to secure communication systems," *Int. J. Bifurc. Chaos*, vol. 3, no. 6, pp. 1619–1627, 1993.

[7] M. J. Ogorzalek, "Taming chaos—Part I: Synchronization," *IEEE Trans. Circuits Syst. I*, vol. 40, pp. 693–699, Oct. 1993.

[8] U. Parlitz, L. O. Chua, L. Kocarev, K. S. Halle, and A. Shang, "Transmission of digital signal by chaotic synchronization," *Int. J. Bifurc. Chaos*, vol. 2, no. 4, pp. 973–977, 1992.

[9] T. L. Carroll, "Communicating with use of filtered, synchronized, chaotic signals," *IEEE Trans. Circuits Syst. I*, vol. 42, pp. 105–110, Mar. 1995.

[10] C. W. Wu and L. O. Chua, "A unified framework for synchronization and control of dynamical systems," *Int. J. Bifurc. Chaos*, vol. 4, no. 4, pp. 979–998, 1994.

[11] ——, "Synchronization in an array of linearly coupled dynamical systems," *IEEE Trans. Circuits Syst. I*, vol. 42, pp. 430–447, Aug. 1995.

[12] L. O. Chua, K. Itoh, L. Kocarev, and K. Eckert, "Chaos synchronization in Chua's circuit," *J. Circuit, Syst. Comput.*, vol. 3, no. 1 pp. 93–108, Mar. 1993.

[13] P. Celka, "Synchronization of chaotic systems though parameter adaption," in *Proc. 1995 IEEE Int. Symp. Circuits Syst.*, Seattle, WA, Apr. 1995, pp. 692–695.

[14] V. N. Belykh, N. N. Verichev, L. Kocarev, and L. O. Chua, "On chaotic synchronization in a linear array of Chua's circuits," *J. Circuit, Syst. Comput.*, vol. 3, no. 2, pp. 579–589, 1993.

[15] K. M. Cuomo, "Synthesizing self-synchronization chaotic arrays," *Int. J. Bifurc. Chaos*, vol. 4, no. 3, pp. 727–736, 1994.

[16] ——, "Synthesizing self-synchronization chaotic systems," *Int. J. Bifurc. Chaos*, vol. 3, no. 5, pp. 1327–1337, 1993.

[17] C. W. Wu, G. Q. Zhong, and L. O. Chua, "Synchronizing nonautonomous chaotic systems without phase-locking," to appear in *J. Circuit, Syst. Comput.*

[18] J. M. Cruz and L. O. Chua, "An IC chip of Chua's circuit," *IEEE Trans. Circuits Syst. II*, vol. 40, pp. 614–625, Oct. 1993.

[19] J. Stark and B. V. Arumugam, "Extracting slowly varying signals from a chaotic background," *Int. J. Bifurc. Chaos*, vol. 2, pp. 413–419, 1992.

[20] T. Yang, "Recovery of digital signals from chaotic switching," *J. Circuit Theory Applicat..*, vol. 23, pp. 611–615, Dec. 1995.

[21] L. O. Chua, "Chua's circuit—An overview ten years later," *J. of Circuit, Syst. Comput.*, vol. 4, no. 2, pp. 117–159, June 1994.

[22] B. A. Huberman and E. Lumer, "Dynamics of adaptive systems," *IEEE Trans. Circuits Syst.*, vol. 37, pp. 547–550, Apr. 1990.

[23] J. K. John and R. E. Amritkar, "Synchronization by feedback and adaptive control," *Int. J. Bifurc. Chaos*, vol. 4, no. 6, pp. 1687–1695, 1994.